Adaptive Sampling for Rapidly Matching Histograms

Stephen Macke[†], Yiming Zhang[‡], Silu Huang[†], Aditya Parameswaran[†]
University of Illinois-Urbana Champaign
[†]{smacke,shuang86,adityagp}@illinois.edu | [‡]ym_zhang@sjtu.edu.cn

ABSTRACT

In exploratory data analysis, analysts often have a need to identify histograms that possess a specific distribution, among a large class of candidate histograms, e.g., find countries whose income distribution is most similar to that of Greece. This distribution could be a new one that the user is curious about, or a known distribution from an existing histogram visualization. At present, this process of identification is brute-force, requiring the manual generation and evaluation of a large number of histograms. We present FastMatch: an end-to-end approach for interactively retrieving the histogram visualizations most similar to a user-specified target, from a large collection of histograms. The primary technical contribution underlying FastMatch is a probabilistic algorithm, HistSim, a theoretically sound sampling-based approach to identify the top-k closest histograms under ℓ_1 distance. While HistSim can be used independently, within FastMatch we couple HistSim with a novel system architecture that is aware of practical considerations, employing asynchronous block-based sampling policies. FastMatch obtains near-perfect accuracy with up to $35\times$ speedup over approaches that do not use sampling on several real-world datasets.

PVLDB Reference Format:
Stephen Macke, Yiming Zhang, Silu Huang, and Aditya Parameswaran. Adaptive Sampling for Rapidly Matching Histograms. *PVLDB*, 11(10): 1262-1275, 2018.
DOI: https://doi.org/10.14778/3231751.3231753

1. INTRODUCTION

In exploratory data analysis, analysts often generate and peruse a large number of visualizations to identify those that *match desired criteria*. This process of iterative "generate and test" occupies a large part of visual data analysis [13, 30, 58], and is often cumbersome and time consuming, especially on very large datasets that are increasingly the norm. This process ends up impeding interaction, preventing exploration, and delaying the extraction of insights.

Motivating Example: Census Data Exploration. Alice is exploring a census dataset consisting of hundreds of millions of tuples, with attributes such as gender, occupation, nationality, ethnicity, religion, adjusted income, net assets, and so on. In particular, she is interested in understanding how applying various filters impacts the relative distribution of tuples with different attribute values. She might ask questions like *Q1:* Which countries have similar distributions of wealth to that of Greece? *Q2:* In the United States, which professions have an ethnicity distribution similar to the profession of doctor? *Q3:* Which (nationality, religion) pairs have a similar distribution of number of children to Christian families in France?

Proceedings of the VLDB Endowment, Vol. 11, No. 10

DOI: https://doi.org/10.14778/3231751.3231753

This example represents a scenario that often arises in exploratory data analysis—finding matches to a specific distribution. The focus of this paper is to *develop techniques for rapidly exploring a large class of histograms to find those that match a user-specified target*.

Referring to *Q1* in our motivating example, a typical workflow used by Alice may be the following: first, pick a country. Generate the corresponding histogram. Does the visualization look similar to that of Greece? If not, pick another, generate it, and repeat. Else, record it, pick another, generate it, and repeat. If only a select few countries have similar distributions, she may spend a huge amount of time sifting through her data, or may simply give up early.

The Need for Approximation. Even if Alice generates all of the candidate histograms (i.e., one for each country) in a single pass, programmatically selecting the closest match to her target (i.e., the Greece histogram), this could take unacceptably long. If the dataset is tens of gigabytes and every tuple in her census dataset contributes to some histogram, then any exact method must necessarily process tens of gigabytes—on a typical workstation, this can take tens of seconds even for in-memory data. Recent work suggests that latencies greater than 500ms cause significant frustration for end-users and lead them to test fewer hypotheses and potentially identify fewer insights [49]. Thus, in this work, we explore approximate techniques that can return matching histogram visualizations with accuracy guarantees, but much faster.

One tempting approach is to employ approximation using pre-computed samples [7, 6, 5, 10, 28, 26], or pre-computed sketches or other summaries [16, 56, 70]. Unfortunately, in an interactive exploration setting, pre-computed samples or summaries are not helpful, since the workload is unpredictable and changes rapidly, with more than half of the queries issued one week completely absent in the following week, and more than 90% of the queries issued one week completely absent a month later [54]. In our case, based on the results for one matching query, Alice may be prompted to explore different (and arbitrary) slices of the same data, which can be exponential in the number of attributes in the dataset. Instead, we materialize samples on-the-fly, which doesn't suffer from the same limitations and has been employed for generating approximate visualizations incrementally [60], and while preserving ordering and perceptual guarantees [42, 8]. To the best of our knowledge, however, on-demand approximate sampling techniques have not been applied to the problem of evaluating a large number of visualizations for matches in parallel.

Key Research Challenges. In developing an approximation-based approach for rapid histogram matching we immediately encounter a number of theoretical and practical challenges.

1. Quantifying Importance. To benefit from approximation, we need to be able to quantify which samples are "important" to facilitate progress towards termination. It is not clear how to assess this importance: at one extreme, it may be preferable to sample more from candidate histograms that are more "uncertain", but these histograms may already be known to be rather far away from the target. Another approach is to sample more from candidate histograms at the "boundary" of top-k, but if these histograms are more "certain", refining them further may be useless. Another challenge is when we quantify the importance of samples: one approach would be to reassess importance every time new data become available, but this approach could be computationally costly.

2. Deciding to Terminate. Our algorithm needs to ascribe a confidence in the correctness of partial results in order to determine when it may safely terminate. This "confidence quantification" requires a statistical test. If we perform this test too often, we spend a significant amount of time doing computation that could be spent performing I/O, and we lose statistical power since we are performing more tests; if we do not perform this test often enough, we may end up taking many more samples than are necessary to terminate.

3. Challenges with Storage Media. When performing sampling from traditional storage media, the cost to fetch samples is locality-dependent; truly random sampling is extremely expensive due to random I/O, while sampling at the level of blocks is much more efficient, but is less random.

4. Communication between Components. It is crucial for our overall system to not be bottlenecked on any component. In particular, the process of quantifying importance (via the sampling manager) must not block the actual I/O performed; otherwise, the time for execution may end up being greater than the time taken by exact methods. As such, these components must proceed asynchronously, while also minimizing communication across them.

Our Contributions. In this paper, we have developed an end-to-end architecture for histogram matching, dubbed FastMatch, addressing the challenges identified above:

1. Importance Quantification Policies. We develop a sampling engine that employs a simple and theoretically well-motivated criterion for deciding whether processing particular portions of data will allow for faster termination. Since the criterion is simple, it is *easy to update* as we process new data, "understanding" when it has seen enough data for some histogram, or when it needs to take more data to distinguish histograms that are close to each other.

2. Termination Algorithm. We develop a statistics engine that repeatedly performs a lightweight "safe termination" test, based on the idea of performing multiple hypothesis tests for which simultaneous rejection implies correctness of the results. Our statistics engine further quantifies how often to run this test to ensure timely termination without sacrificing too much statistical power.

3. Locality-aware Sampling. To better exploit locality of storage media, FastMatch samples at the level of blocks, proceeding sequentially. To estimate the benefit of blocks, we leverage bitmap indexes in a cache-conscious manner, evaluating multiple blocks at a time in the same order as their layout in storage. Our technique minimizes the time required for the query output to satisfy our probabilistic guarantees.

4. Decoupling Components. Our system decouples the overhead of deciding which samples to take from the actual I/O used to read the samples from storage. In particular, our sampling engine utilizes a just-in-time lookahead technique that marks blocks for reading or skipping while the I/O proceeds unhindered, in parallel.

Overall, we implement FastMatch within the context of a bitmap-based sampling engine, which allows us to quickly determine whether a given memory or disk block could contain samples matching ad-hoc predicates. Such engines were found to effectively support approximate generation of visualizations in recent work [8, 42, 60].

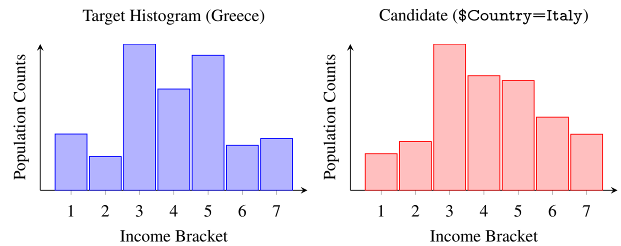

Figure 1: Example visual target and candidate histogram

We find that our approximation-based techniques working in tandem with our novel systems components ***lead to speedups ranging from*** $8\times$ ***to over*** $35\times$ over exact methods, and moreover, unlike less-sophisticated variants of FastMatch, whose performance can be highly data-dependent, FastMatch consistently brings latency to near-interactive levels.

Related Work. To the best of our knowledge, there has been no work on sampling to identify histograms that match user specifications. Sampling-based techniques have been applied to generate visualizations that preserve visual properties [8, 42], and for incremental generation of time-series and heat-maps [60]—all focusing on the generation of a single visualization. Similarly, Pangloss [53] employs approximation via the Sample+Seek approach [26] to generate a single visualization early, while minimizing error. M4 uses rasterization without sampling to reduce the dimensionality of a time-series visualization and generate it faster [40]. SeeDB [65] recommends visualizations to help distinguish between two subsets of data while employing approximation. However, their techniques are tailored to evaluating differences between pairs of visualizations (that share the same axes, while other pairs do not share the same axes). In our case, we need to compare one visualization versus others, all of which have the same axes and have comparable distances, hence the techniques do not generalize.

Recent work has developed zenvisage [62], a visual exploration tool, including operations that identify visualizations similar to a target. However, to identify matches, zenvisage does not consider sampling, and requires at least one complete pass through the dataset. FastMatch was developed as a back-end with such interfaces in mind to support rapid discovery of relevant visualizations. Additional related work is surveyed in Section 6.

2. PROBLEM FORMULATION

In this section, we formalize the problem of identifying histograms whose distributions match a reference.

2.1 Generation of Histograms

We start with a concrete example of the typical database query an analyst might use to generate a histogram. Returning to our example from Section 1, suppose an analyst is interested in studying how population proportions vary across income brackets for various countries around the world. Suppose she wishes to find countries with populations distributed across different income brackets most similarly to a specific country, such as Greece. Consider the following SQL query, where $COUNTRY is a variable:

```
SELECT income_bracket, COUNT(*) FROM census
WHERE country=$COUNTRY
GROUP BY income_bracket
```

This query returns a list of 7 (income bracket, count) pairs to the analyst for a specific country. The analyst may then choose to visualize the results by plotting the counts versus different income brackets in a histogram, i.e., a plot similar to the right side of Figure 1 (for Italy). Currently, the analyst may examine hundreds of

Table 1: Summary of notation.

Symbol(s)	Description
X, Z, V_X, V_Z, T	x-axis attribute, candidate attribute, respective value sets, and relation over these attributes, used in histogram-generating queries (see Definition 1)
$k, \delta, \varepsilon, \sigma$	User-supplied parameters (number of matching histograms to retrieve, error probability upper bound, approximation error upper bound, selectivity threshold (below which candidates may optionally be ignored)
$\mathbf{q}, \mathbf{r}_i, \mathbf{r}_i^*, (\bar{\mathbf{q}}, \bar{\mathbf{r}}_i, \bar{\mathbf{r}}_i^*)$	Visual target, candidate i's estimated (unstarred) and true (starred) histogram counts (normalized variants)
$d(\cdot, \cdot)$	Distance function, used to quantify visual distance (see Definition 2)
$n_i, n_i', \varepsilon_i, \delta_i, \tau_i\ (\tau_i^*)$	Quantities specific to candidate i during HistSim run: number of samples taken, estimated samples needed (see Section 4), deviation bound (see Definition 4), confidence upper bound on ε_i-deviation or rareness, and distance estimate from $\mathbf{q}$ (true distance from $\mathbf{q}$), respectively
$n_i^\partial, \mathbf{r}_i^\partial, \tau_i^\partial$	Quantities corresponding to samples taken in a specific round of HistSim stage 2: number of samples taken for candidate i in round, per-group counts for candidate i for samples taken in round, corresponding distance estimates using the samples taken in round, respectively
M, A	Set of matching histograms (see Definition 3) and non-pruned histograms, respectively, during a run of HistSim
$N_i, N, m, f(\cdot; N, N_i, m)$	Number of datapoints corresponding to candidate i, total number of datapoints, samples taken during stage 1, hypergeometric pdf

similar histograms, one for each country, comparing it to the one for Greece, to manually identify ones that are similar.

In contrast, the goal of FastMatch is to perform this search automatically and efficiently. Conceptually, FastMatch will iterate over all possible values of country, generate the corresponding histograms, and evaluate the similarity of its distribution (based on some notion of similarity described subsequently) to the corresponding visualization for Greece. In actuality, FastMatch will perform this search all at once, quickly pruning countries that are either clearly close or far from the target.

Candidate Visualizations. Formally, we consider visualizations as being generated as a result of **histogram-generating queries**:

DEFINITION 1. *A* histogram-generating query *is a SQL query of the following type:*

SELECT X, COUNT(*) FROM T
WHERE $Z = z_i$ GROUP BY X

The table T and attributes X and Z form the query's template.

For each concrete value z_i of attribute Z specified in the query, the results of the query—i.e., the grouped counts—can be represented in the form of a vector $(r_1, r_2, \ldots, r_n)$, where $n = |V_X|$, the cardinality of the value set of attribute X. This n-tuple can then be used to plot a histogram visualization—in this paper, when we refer to a histogram or a visualization, we will be typically referring to such an n-tuple. For a given *grouping attribute* X and a *candidate attribute* Z, we refer to the set of all visualizations generated by letting Z vary over its value set as the set of ***candidate visualizations***. We refer to each distinct value in the grouping attribute X's value set as a *group*. In our example, X corresponds to `income_bracket` and Z corresponds to `country`.

For ease of exposition, we focus on candidate visualizations generated from queries according to Definition 1, having single categorical attributes for X and Z. Our methods are more general and extend naturally to handle *(i) predicates:* additional predicates on other attributes, *(ii) multiple and complex Xs:* additional grouping (i.e., X) attributes, groups derived from binning real-values (as opposed to categorical X), along with groups derived from binning multiple categorical X attribute values together (e.g., quarters instead of individual months), and *(iii) multiple and complex Zs:* additional candidate (i.e., Z) attributes, as well as candidate attribute values derived from binning real values (as opposed to categorical Z). We discuss these extensions in our technical report [51]. The flexibility in specifying histogram-generating queries—exponential in the number of attributes—makes it impossible for us to precompute the results of all such queries.

Visualization Terminology. Our methods are agnostic to the particular method used to present visualizations. That is, analysts may choose to present the results generated from queries of the form in Definition 1 via line plots, heat maps, choropleths, and other visualization types, as any of these may be specified by an ordered tuple of real values and are thus permitted under our notion of a "candidate visualization". We focus on bar charts of frequency counts and histograms—these naturally capture aggregations over the categorical or binned quantitative grouping attribute X respectively. Although a bar graph plot of frequency counts over a categorical grouping attribute is not technically a histogram, which implies that the grouping attribute is continuous, we loosely use the term "histogram" to refer to both cases in a unified way.

Visual Target Specification. Given our specification of candidate visualizations, a ***visual target*** is an n-tuple, denoted by $\mathbf{q}$ with entries $Q_1, Q_2, \ldots, Q_n$, that we need to match the candidates with. Returning to our flight delays example, $\mathbf{q}$ would refer to the visualization corresponding to Greece, with Q_1 being the count of individuals in the first income bracket, Q_2 the count of individuals in the second income bracket, and so on.

Samples. To estimate these candidate visualizations, we need to take *samples*. In particular, for a given candidate i for some attribute Z, a sample corresponds to a single tuple t with attribute value $Z = z_i$. The attribute value $X = x_j$ of t increments the jth entry of the estimate $\mathbf{r}_i$ for the candidate histogram.

Candidate Similarity. Given a set of candidate visualizations with estimated vector representations $\{\mathbf{r}_i\}$ such that the ith candidate is generated by selecting on $Z = z_i$, our problem hinges on finding the candidate whose distribution is most "similar" to the visual target $\mathbf{q}$ specified by the analyst. For quantifying visual similarity, we do not care about the absolute counts $r_1, r_2, \ldots, r_{|V_X|}$, and instead prefer to determine whether $\mathbf{r}_i$ and $\mathbf{q}$ are close in a *distributional* sense. Using hats to denote normalized variants of $\mathbf{r}_i$ and $\mathbf{q}$, write

$$\bar{\mathbf{r}}_i = \frac{\mathbf{r}_i}{\mathbf{1}^T\mathbf{r}_i} \qquad \bar{\mathbf{q}} = \frac{\mathbf{q}}{\mathbf{1}^T\mathbf{q}}$$

With this notational convenience, we make our notion of similarity explicit by defining candidate distance as follows:

DEFINITION 2. *For candidate $\mathbf{r}_i$ and visual predicate $\mathbf{q}$, the* ***distance*** *$d(\mathbf{r}_i, \mathbf{q})$ between $\mathbf{r}_i$ and $\mathbf{q}$ is defined as follows:*

$$d(\mathbf{r}_i, \mathbf{q}) = ||\bar{\mathbf{r}}_i - \bar{\mathbf{q}}||_1 = ||\frac{\mathbf{r}_i}{\mathbf{1}^T\mathbf{r}_i} - \frac{\mathbf{q}}{\mathbf{1}^T\mathbf{q}}||_1$$

That is, after normalizing the candidate and target vectors so that their respective components sum to 1 (and therefore correspond to distributions), we take the ℓ_1 distance between the two vectors. When the target $\mathbf{q}$ is understood from context, we denote the distance between candidate $\mathbf{r}_i$ and $\mathbf{q}$ by $\tau_i = d(\mathbf{r}_i, \mathbf{q})$.

The Need for Normalization. A natural question that readers may have is why we chose to normalize each vector prior to taking the distance between them. We do this because the goal of FastMatch is to find visualizations that have similar distributions, as opposed to similar actual values. Returning to our example, if we consider the population distribution of Greece across different income brackets, and compare it to that of other countries, without normalization, we will end up returning other countries with similar population counts in each bin—e.g., other countries with similar overall populations—as opposed to those that have similar shape or distribution. A similar metric, using ℓ_2 distance between normalized vectors (as opposed to ℓ_1), has been studied in prior work [65, 26] and even validated in a user study in [65]. However, as observed in [12], the ℓ_2 distance between distributions has the drawback that it could be small even for distributions with disjoint support. The ℓ_1 distance metric over discrete probability distributions has a direct correspondence with the traditional statistical distance metric known as *total variation distance* [29] and does not suffer from this drawback, so we prefer it in this work.

2.2 Guarantees and Problem Statement

FastMatch takes samples to estimate the candidate histogram visualizations. Since FastMatch is approximate, we need to enforce probabilistic guarantees on the correctness of the returned results.

First, we introduce some notation: we use $\mathbf{r}_i$ to denote the *estimate* of the candidate visualization, while $\mathbf{r}_i^*$ (with normalized version $\overline{\mathbf{r}}_i^*$) is the *true* candidate visualization on the entire dataset. Our formulation also relies on constants ε, δ, and σ, which we assume either built into the system or provided by the analyst. We further use N and N_i to denote the total number of datapoints and number of datapoints corresponding to candidate i, respectively.

GUARANTEE 1. (SEPARATION) *Any approximate histogram $\mathbf{r}_i$ with selectivity $\frac{N_i}{N} \geq \sigma$ that is in the true top-k closest (w.r.t. Definition 2) but* not *part of the output will be less than ε closer to the target than the furthest histogram that* is *part of the output. That is, if the algorithm outputs histograms $\mathbf{r}_{j_1}, \mathbf{r}_{j_2}, \ldots, \mathbf{r}_{j_k}$, then, for all i, $\max_{1\leq l\leq k}\left\{d(\mathbf{r}_{j_l}^*, \mathbf{q})\right\} - d(\mathbf{r}_i^*, \mathbf{q}) < \varepsilon$, or $\frac{N_i}{N} < \sigma$.*

GUARANTEE 2. (RECONSTRUCTION) *Each approximate histogram $\mathbf{r}_i$ output as one of the top-k satisfies $d(\mathbf{r}_i, \mathbf{r}_i^*) < \varepsilon$.*

The first guarantee says that any ordering mistakes are relatively innocuous: for any two histograms $\mathbf{r}_i$ and $\mathbf{r}_j$, if the algorithm outputs $\mathbf{r}_j$ but not $\mathbf{r}_i$, when it should have been the other way around, then either $\left|d(\mathbf{r}_i^*, \mathbf{q}) - d(\mathbf{r}_j^*, \mathbf{q})\right| < \varepsilon$, or $\frac{N_i}{N} < \sigma$. The intuition behind the minimum selectivity parameter, σ, is that certain candidates may not appear frequently enough within the data to get a reliable reconstruction of the true underlying distribution responsible for generating the original data, and thus may not be suitable for downstream decision-making. In our income example, a country with a population of 100 may have a histogram similar to the visual target, but this would not be statistically significant. Overall, our guarantee states that we still return a histogram that is close to $\mathbf{q}$, and we can be confident that anything much closer has relatively few total datapoints appearing in the data (i.e., N_i is small).

The second guarantee says that the histograms output are not too dissimilar from the corresponding true distributions that would result from a complete scan of the data. Thus, they form an adequate and accurate proxy from which insights may be derived. With these definitions in place, we now formally state our core problem:

PROBLEM 1. (TOP-K-SIMILAR). *Given a visual target $\mathbf{q}$, a histogram-generating query template, k, ε, δ, and σ, display k candidate attribute values $\{z_i\} \subseteq V_Z$ (and accompanying visualizations $\{\mathbf{r}_i\}$) as quickly as possible, such that the output satisfies Guarantees 1 and 2 with probability greater than $1-\delta$.*

3. THE HISTSIM ALGORITHM

In this section, we discuss how to conceptually solve Problem 1. We outline an algorithm, named HistSim, which allows us to determine confidence levels for whether our separation and reconstruction guarantees hold. We rigorously prove in this section that when our algorithm terminates, it gives correct results with probability greater than $1-\delta$ *regardless* of the data given as input. Many systems-level details and other heuristics used to make HistSim perform particularly well in practice will be presented in Section 4. Table 1 provides a description of the notation used. All proofs appearing in this section can be found in our technical report [51].

Algorithm 1: The HistSim algorithm

Input : Columns Z, X, visual target $\mathbf{q}$, parameters $k, \varepsilon, \delta, \sigma$
Output : Estimates M of the top-k closest candidates to $\mathbf{q}$, histograms $\{\mathbf{r}_i\}$

Initialization.
$n_i, n_i^{\partial} \leftarrow 0, \mathbf{r}_i, \mathbf{r}_i^{\partial} \leftarrow \mathbf{0}$ for $1 \leq i \leq |V_Z|$;

stage 1: $\delta^{upper} \leftarrow \frac{\delta}{3}$;
Repeat m times: uniformly randomly sample some tuple without replacement;
Update $\{n_i\}, \{\mathbf{r}_i\}, \{\tau_i\}$ based on the new samples;
$\Delta \leftarrow \{\delta_i\}$ where $\delta_i = \sum_{j=0}^{n_i} f(j; N, \lceil\sigma N\rceil, m)$ for $1 \leq i \leq |V_Z|$;
Perform a Holm-Bonferroni statistical test with P-values in Δ; that is:
$A \leftarrow \left\{i : \delta_i \leq \frac{\delta}{|V_Z|-i+1} \text{ and for all } j < i, \delta_j \leq \frac{\delta}{|V_Z|-j+1}\right\}$;

stage 2: $\delta^{upper} \leftarrow \frac{\delta}{3}$;
do
  $\delta^{upper} \leftarrow \frac{1}{2}\delta^{upper}$;
  $n_i \mathrel{+}= n_i^{\partial}, \quad \mathbf{r}_i \mathrel{+}= \mathbf{r}_i^{\partial}, \quad \tau_i \leftarrow d(\mathbf{r}_i, \mathbf{q}) \quad$ for $i \in A$;
  $n_i^{\partial} \leftarrow 0, \quad \mathbf{r}_i^{\partial} \leftarrow \mathbf{0} \quad$ for $i \in A$;
  $M \leftarrow \{i \in A : \tau_i$ among k smallest$\}$;
  $s \leftarrow \frac{1}{2}(\max_{i\in M}\tau_i + \min_{j\in A\setminus M}\tau_j)$;
  Repeat: take uniform random samples from any $i \in A$;
  Update $\{n_i^{\partial}\}, \{\mathbf{r}_i^{\partial}\}$, and $\{\tau_i^{\partial}\}$ based on the new samples;
  $\varepsilon_i \leftarrow s + \frac{\varepsilon}{2} - \tau_i^{\partial}$ for $i \in M$;
  $\varepsilon_j \leftarrow \tau_j^{\partial} - (s - \frac{\varepsilon}{2})$ if $s - \frac{\varepsilon}{2} \geq 0$ else ∞ for $j \in A \setminus M$;
  $\Delta \leftarrow \{\delta_i\}$ where $\delta_i \geq \mathbb{P}\left(d(\mathbf{r}_i^{\partial}, \mathbf{r}_i^*) > \varepsilon_i\right)$ for $i \in A$;
while $\max(\Delta) > \delta^{upper}$;

stage 3: Sample until $n_i \geq \frac{2}{\varepsilon^2}\left(|V_X|\log 2 + \log\frac{3k}{\delta}\right)$, for all $i \in M$;
Update $\{\mathbf{r}_i\}$ based on the new samples;
return M, *and* $\{\mathbf{r}_i : i \in M\}$;

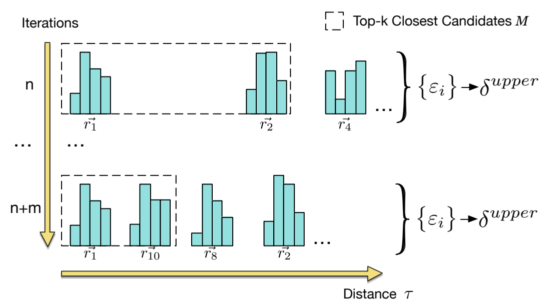

Figure 2: Illustration of HistSim.

3.1 Algorithm Outline

HistSim operates by sampling tuples. Each of these tuples contributes to one or more candidate histograms, using which HistSim constructs histograms $\{\overline{\mathbf{r}}_i\}$. After taking enough samples corresponding to each candidate, it will eventually be likely that $d(\mathbf{r}_i, \mathbf{r}_i^*)$ is "small", and that $|d(\mathbf{r}_i, \mathbf{q}) - d(\mathbf{r}_i^*, \mathbf{q})|$ is likewise "small", for each i. More precisely, the set of candidates will likely be in a state such that Guarantees 1 and 2 are both satisfied simultaneously.

Stages Overview. HistSim separates its sampling into three stages, each with an error probability of at most $\frac{\delta}{3}$, giving an overall error probability of at most δ:

- Stage 1 [Prune Rare Candidates]: Sample datapoints uniformly at random without replacement, so that each candidate is sampled a number of times roughly proportional to the number of datapoints corresponding to that candidate. Identify rare candidates that likely satisfy $\frac{N_i}{N} < \sigma$, and prune these ones.
- Stage 2 [Identify Top-k]: Take samples from the remaining candidates until the top-k have been identified reliably.
- Stage 3 [Reconstruct Top-k]: Sample from the estimated top-k until they have been reconstructed reliably.

This separation is important for performance: the pruning step (stage

1) often *dramatically reduces* the number of candidates that need to be considered in stages 2 and 3.

The first two stages of HistSim factor into phases that are pure I/O and phases that involve one or more statistical tests. The I/O phases sample tuples (lines 6 and 19 in Algorithm 1)—we will describe how in Section 4; our algorithm's correctness is independent of how this happens, provided that the samples are uniform.

Stage 1: Pruning Rare Candidates (Section 3.3). During stage 1, the I/O phase (line 6) takes m samples, for some m fixed ahead of time. This is followed by updating, for each candidate i, the number of samples n_i observed so far (line 7), and using the P-values $\{\delta_i\}$ of a test for underrepresentation to determine whether each candidate i is rare, i.e., has $\frac{N_i}{N} < \sigma$ (lines 7–9).

Stage 2: Identifying Top-k (Section 3.4). For stage 2, we focus on a smaller set of candidates; namely, those that we did not find to be rare (denoted by A). Stage 2 is divided into *rounds*. Each round attempts to use existing samples to estimate which candidates are top-k and which are non top-k, and then draws new samples, testing how unlikely it is to observe the new samples in the event that its guess of the top-k is wrong. If this event is unlikely enough, then it has recovered the correct top-k, with high probability.

At the start of each round, HistSim accumulates any samples taken during the previous round (lines 15–16). It then determines the current top-k candidates and a separation point s between top-k and non top-k (lines 17–18), as this separation point determines a set of hypotheses to test. Then, it begins an I/O phase and takes samples (line 19). The samples taken each round are used to generate the number of samples taken per candidate, $\{n_i^\partial\}$, the estimates $\{\mathbf{r}_i^\partial\}$, and the distance estimates $\{\tau_i^\partial\}$ (line 20). These statistics are computed from fresh samples each round (i.e., they do not reuse samples across rounds) so that they may be used in a statistical test (lines 20–23), discussed in Section 3.4. After computing the P-values for each null hypothesis to test (line 23), HistSim determines whether it can reject all the hypotheses with type 1 error (i.e., probability of mistakenly rejecting a true null hypothesis) bounded by δ^{upper} and break from the loop (line 24). If not, it repeats with new samples and a smaller δ^{upper} (where the $\{\delta^{upper}\}$ are chosen so that the probability of error across *all* rounds is at most $\frac{\delta}{3}$).

Stage 3: Reconstructing Top-k (Section 3.5). Finally, stage 3 ensures that the identified top-k, M, all satisfy $d(\mathbf{r}_i, \mathbf{r}_i^*) \leq \varepsilon$ for $i \in M$ (so that Guarantee 2 holds), with high probability.

Figure 2 illustrates HistSim stage 2 running on a toy example in which we compute the top-2 closest histograms to a target. At round n, it estimates $\mathbf{r}_1$ and $\mathbf{r}_2$ as the top-2 closest, which it refines by the time it reaches round $n + m$. As the rounds increase, HistSim takes more samples to get better estimates of the distances $\{\tau_i\}$ and thereby improve the chances of termination when it performs its multiple hypothesis test in stage 2.

Choosing where to sample and how many samples to take. The estimates M and $\{\tau_i\}$ allow us to determine which candidates are "important" to sample from in order to allow termination with fewer samples; we return to this in Section 4. Our HistSim algorithm is agnostic to the sampling approach.

Outline. We first discuss the Holm-Bonferroni method for testing multiple statistical hypotheses simultaneously in Section 3.2, since stage 1 of HistSim uses it as a subroutine, and since the simultaneous test in stage 2 is based on similar ideas. In Section 3.3, we discuss stage 1 of HistSim, and prove that upon termination, all candidates i flagged for pruning satisfy $\frac{N_i}{N} < \sigma$ with probability greater than $\frac{\delta}{3}$. Next, in Section 3.4, we discuss stage 2 of HistSim, and prove that upon termination, we have the guarantee that any non-pruned candidate mistakenly classified as top-k is no more than ε further from the target than the furthest true non-pruned top-k candidate (with high probability). The proof of correctness for stage 2 is the most involved and is divided as follows:

- In Section 3.4.1, we give lemmas that allow us to relate the reconstruction of the candidate histograms from estimates $\{\mathbf{r}_i^\partial\}$ to the separation guarantee via multiple hypothesis testing;
- In Section 3.4.2, we describe a method to select appropriate hypotheses to use for testing in the lemmas of Section 3.4.1;
- In Section 3.4.3, we prove a theorem that enables us to use the samples per candidate histogram to determine the P-values associated with the hypotheses.

In Section 3.5, we discuss stage 3 and conclude with an overall proof of correctness.

3.2 Controlling Family-wise Error

In the first two stages of HistSim, the algorithm needs to perform multiple statistical tests simultaneously [15]. In stage 1, HistSim tests null hypotheses of the form "candidate i is high-selectivity" versus alternatives like "candidate i is not high-selectivity". In this case, "rejecting the null hypothesis at level δ^{upper}" roughly means that the probability that candidate i is high-selectivity is at most δ^{upper}. Likewise, during stage 2, HistSim tests null hypotheses of the form "candidate i's true distance from $\mathbf{q}$, τ_i^*, lies above (or below) some fixed value s." If the algorithm correctly rejects every null hypothesis while controlling the family-wise error [45] at level δ^{upper}, then it has correctly determined which side of s every τ_i^* lies, a fact that we use to get the separation guarantee.

Since stages 1 and 2 test multiple hypotheses at the same time, HistSim needs to control the family-wise type 1 error (false positive) rate of these tests simultaneously. That is, if the family-wise type 1 error is controlled at level δ^{upper}, then the probability that one or more rejecting tests in the family should not have rejected is less than δ^{upper} — during stage 1, this intuitively means that the probability one or more high-selectivity candidates were deemed to be low-selectivity is at most δ^{upper}, and during stage 2, this roughly means that the probability of selecting some candidate as top-k when it is non top-k (or vice-versa) is at most δ^{upper}.

The reader may be familiar with the Bonferroni correction, which enforces a family-wise error rate of δ^{upper} by requiring a significance level $\frac{\delta^{upper}}{|V_Z|}$ for each test in a family with $|V_Z|$ tests in total. We instead use the Holm-Bonferroni method [33], which is uniformly more powerful than the Bonferroni correction, meaning that it needs fewer samples to make the same guarantee. In brief, a level δ^{upper} test over a family of size $|V_Z|$ works by first sorting the P-values $\{\delta_i\}$ of the individual tests in increasing order, and then finding the minimal index j (starting from 1) where $\delta_j > \frac{\delta^{upper}}{|V_Z|-j+1}$ (if this does not exist, then set $j = |V_Z|$). The tests with smaller indices reject their respective null hypotheses at level δ^{upper}, and the remaining ones do not reject.

3.3 Stage 1: Pruning Rare Candidates

To prune rare candidates, we need some way to determine whether each candidate i satisfies $\frac{N_i}{N} < \sigma$ with high probability. To do so, we make the simple observation that, after drawing m tuples without replacement uniformly at random, the number of tuples corresponding to candidate i follows a hypergeometric distribution [39]. The number of samples to take, m, is a parameter; we observe in our experiments that $m = 5 \cdot 10^5$ is an appropriate choice.[1] That is, if candidate i has N_i total corresponding tuples in a dataset of size N, then the number of tuples n_i for candidate i in a uniform sample without replacement of size m is distributed according to $n_i \sim \text{HypGeo}(N, N_i, m)$. As such, we can make use of

[1]Our results are not sensitive to the choice of m, provided m is not too small (so that the algorithm fails to prune anything) or too big (i.e., a nontrivial fraction of the data).

a well-known test for underrepresentation [45] to accurately detect when candidate i has $\frac{N_i}{N} < \sigma$. The null hypothesis is that candidate i is not underrepresented (i.e., has $N_i \geq \sigma N$), and letting $f(\,\cdot\,; N, \lceil \sigma N \rceil, m)$ denote the hypergeometric pdf in this case, the P-value for the test is given by $\sum_{j=0}^{n_i} f(j; N, \lceil \sigma N \rceil, m)$, where n_i is the number of observed tuples for candidate i in the sample of size m. Roughly speaking, the P-value measures how surprised we are to observe n_i or fewer tuples for candidate i when $\frac{N_i}{N} \geq \sigma$ — the lower the P-value, the more surprised we are.

If we reject the null hypothesis for some candidate i when the P-value is at most δ_i, we are claiming that candidate i satisfies $\frac{N_i}{N} < \sigma$, and the probability that we are wrong is then at most δ_i. Of course, we need to test *every* candidate for rareness, not just a given candidate, which is why HistSim stage 1 uses a Holm-Bonferroni procedure to control the *family-wise* error at any given threshold.

We now prove a lemma regarding correctness of stage 1.

LEMMA 1 (STAGE 1 CORRECTNESS). *After* HistSim *stage 1 completes, every candidate i removed from A satisfies $\frac{N_i}{N} < \sigma$, with probability greater than $1 - \frac{\delta}{3}$*

The proof is a consequence of the correctness of each individual test for underrepresentation in conjunction with the correctness of the Holm-Bonferroni procedure for family-wise error [51].

3.4 Stage 2: Identifying Top-K Candidates

HistSim stage 2 attempts to find the top-k closest to the target out of those remaining after stage 1. To facilitate discussion, we first introduce some definitions.

DEFINITION 3. *(*MATCHING CANDIDATES*) A candidate is called* matching *if its distance estimate $\tau_i = d(\mathbf{r}_i, \mathbf{q})$ is among the k smallest out of all candidates remaining after stage 1.*

We denote the (dynamically changing) set of candidates that are matching during a run of HistSim as M; we likewise denote the true set of matching candidates out of the remaining, non-pruned candidates in A as M^*. Next, we introduce the notion of ε_i*-deviation*.

DEFINITION 4. *(*ε_i-DEVIATION*) The empirical vector of counts $\mathbf{r}_i$ for some candidate i has ε_i-deviation if the corresponding normalized vector $\bar{\mathbf{r}}_i$ is within ε_i of the exact distribution $\bar{\mathbf{r}}_i^*$. That is, $d(\mathbf{r}_i, \mathbf{r}_i^*) = ||\bar{\mathbf{r}}_i - \bar{\mathbf{r}}_i^*||_1 < \varepsilon_i$*

Note that Definition 4 overloads the symbol ε to be candidate-specific by appending a subscript. In Section 3.4.3, we provide a way to quantify ε_i given samples.

If HistSim reaches a state where, for each matching candidate $i \in M$, candidate i has ε_i-deviation, and $\varepsilon_i < \varepsilon$ for all $i \in M$, then it is easy to see that the Guarantee 2 holds for the matching candidates. That is, in such a state, if HistSim output the histograms corresponding to the matching candidates, they would look similar to the true histograms. In the following sections, we show that ε_i-deviation can also be used to achieve Guarantee 1.

3.4.1 Deviation-Bounds Imply Separation

In order to reason about the separation guarantee, we prove a series of lemmas following the structure of reasoning given below:

- We show that when a carefully chosen set of null hypotheses are all false, M contains valid top-k closest candidates.
- Next, we show how to use ε_i-deviation to upper bound the probability of rejecting a *single* true null hypothesis.
- Finally, we show how to reject *all* null hypotheses while controlling the probability of rejecting *any* true ones.

LEMMA 2 (FALSE NULLS IMPLY SEPARATION). *Consider the set of null hypotheses $\{H_0^{(i)}\}$ defined as follows, where $s \in \mathbb{R}^+$:*

$$H_0^{(i)} = \begin{cases} \tau_i^* \geq s + \frac{\varepsilon}{2}, \textit{ for } i \in M \\ \tau_i^* \leq s - \frac{\varepsilon}{2}, \textit{ for } i \in A \setminus M \end{cases}$$

When $H_0^{(i)}$ is false for every $i \in A$, then M is a set of top-k candidates that is correct with respect to Guarantee 1.

Intuitively, Lemma 2 states that when there is some reference point s such that all of the candidates in M have their τ_i^* smaller than $s - \frac{\varepsilon}{2}$, and the rest have their τ_i^* greater than $s + \frac{\varepsilon}{2}$, then we have our separation guarantee.

Next, we show how to compute P-values for a single null hypothesis of the type given in Lemma 2. Below, we use "$\mathbb{P}_H$" to denote the probability of some event when hypothesis H is true.

LEMMA 3 (DISTANCE DEVIATION TESTING). *Let $x \in \mathbb{R}^+$. To test the null hypothesis $H_0^{(i)} : \tau_i^* \geq x$ versus the alternative $H_A^{(i)} : \tau_i^* < x$, we have that, for any $\varepsilon_i > 0$,*

$$\mathbb{P}_{H_0^{(i)}}\left[x - \tau_i^\partial > \varepsilon_i\right] \leq \mathbb{P}\left(d(\mathbf{r}_i^\partial, \mathbf{r}_i^*) > \varepsilon_i\right)$$

Likewise, for testing $H_0^{(i)} : \tau_i^* \leq x$ versus the alternative $H_A^{(i)} : \tau_i^* > x$, we have $\mathbb{P}_{H_0^{(i)}}\left[\tau_i^\partial - x > \varepsilon_i\right] \leq \mathbb{P}\left(d(\mathbf{r}_i^\partial, \mathbf{r}_i^*) > \varepsilon_i\right)$.

We use Lemma 3 in conjunction with Lemma 2 by using $s \pm \frac{\varepsilon}{2}$ for the reference x of Lemma 3, for a particular choice of s (discussed in Section 3.4.2). For example, Lemma 3 shows that when we are testing the null hypothesis for $i \in M$ that $\tau_i^* \geq s + \frac{\varepsilon}{2}$ and we observe τ_i^∂ such that $0 < \varepsilon_i = s + \frac{\varepsilon}{2} - \tau_i^\partial$, we can use (any upper bound of) $\mathbb{P}\left(d(\mathbf{r}_i^*, \mathbf{r}_i^\partial) > \varepsilon_i\right)$ as a P-value for this test. That is, consider a tester with the following behavior, illustrated pictorially:

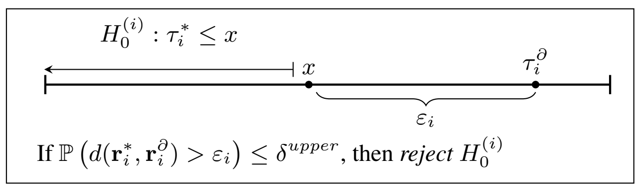

In the above picture, the tester assumes that τ_i^* is smaller than x, but it observes a value τ_i^∂ that exceeds x by ε_i. When the true value $\tau_i^* \leq x$ for any reference x, then the observed statistic τ_i^∂ will only be ε_i or larger than x (and vice-versa) when the reconstruction $\mathbf{r}_i^\partial$ is also bad, in the sense that $\mathbb{P}\left(d(\mathbf{r}_i^*, \mathbf{r}_i^\partial) > \varepsilon_i\right)$ is very small. If the above tester rejects $H_0^{(i)}$ when $\mathbb{P}\left(d(\mathbf{r}_i^*, \mathbf{r}_i^\partial) > \varepsilon_i\right) \leq \delta^{upper}$, then Lemma 3 says that it is guaranteed to reject a true null hypothesis with probability at most δ^{upper}. We discuss how to compute an upper bound on $\mathbb{P}\left(d(\mathbf{r}_i^*, \mathbf{r}_i^\partial) > \varepsilon_i\right)$ in Section 3.4.3.

Finally, notice that Lemma 3 provides a test which controls the type 1 error of an individual $H_0^{(i)}$, but we only know that the separation guarantee holds for $i \in M$ when *all* the hypotheses $\{H_0^{(i)}\}$ are false. Thus, the algorithm requires a way to control the type 1 error of a procedure that decides whether to reject every $H_0^{(i)}$ simultaneously. In the next lemma, we give such a tester which controls the error for any upper bound δ^{upper}. Our tester is essentially the intersection-union method [15] formulated in terms of P-values.

LEMMA 4 (SIMULTANEOUS REJECTION). *Consider any set of null hypotheses* $\{H_0^{(i)}\}$*, and consider a set of P-values* $\{\delta_i\}$ *associated with these hypotheses. The tester given by*

$$\textit{Decision} = \begin{cases} \textit{reject every } H_0^{(i)}, & \textit{when } \max_i \delta_i \le \delta^{upper} \\ \textit{reject no } H_0^{(i)}, & \textit{otherwise} \end{cases}$$

rejects ≥ 1 *true null hypotheses with probability* $\le \delta^{upper}$.

3.4.2 Selecting Each Round's Tests

Each round of HistSim stage 2 constructs a family of tests to perform whose family-wise error probability is at most δ^{upper}. At round t (starting from $t = 1$), δ^{upper} is chosen to be $\frac{\delta/3}{2^t}$, so that the error probability across *all* rounds is at most $\sum_{t\ge 1} \frac{\delta/3}{2^t} = \frac{\delta}{3}$ via a union bound (see Lemma 5 for details).

There is still one degree of freedom: namely, how to choose the split point s used for the null hypotheses in Lemma 2. In line 18, it is chosen to be $s \leftarrow \frac{1}{2}(\max_{i\in M} \tau_i + \min_{j\in A\setminus M} \tau_j)$. The intuition for this choice is as follows. Although the quantities $\mathbf{r}_i^\partial$ and τ_i^∂ are generated from fresh samples in each round of HistSim stage 2, the quantities $\mathbf{r}_i$ and τ_i are generated from samples taken across *all* rounds of HistSim stage 2. As such, as rounds progress (i.e., if the testing procedure fails to simultaneously reject multiple times), the estimates $\mathbf{r}_i$ and τ_i become closer to $\mathbf{r}_i^*$ and τ_i^*, the set M becomes more likely to coincide with M^*, and the null hypotheses $\{H_0^{(i)}\}$ chosen become less likely to be true *provided* an s chosen somewhere in $[\max_{i\in M} \tau_i, \min_{j\in A\setminus M} \tau_j]$, since values in this interval are likely to correctly separate M^* and $A \setminus M^*$ as more and more samples are taken. In the interest of simplicity, we simply choose the midpoint halfway between the furthest candidate in M and the closest candidate in $A\setminus M$. In practice, we observe that $\max_{i\in M} \tau_i$ and $\min_{j\in A\setminus M} \tau_j$ are typically very close to each other, so that the algorithm is not very sensitive to the choice of s.Once s is chosen, the $\{\varepsilon_j\}$ (i.e., the amounts by which the $\{\tau_j^\partial\}$ deviate from $s \pm \frac{\varepsilon}{2}$) determine the P-values associated with the $\{H_0^{(i)}\}$ which ultimately determine whether HistSim stage 2 can terminate, as we discuss more in the next section.

3.4.3 Deviation-Bounds Given Samples

The previous section provides us a way to check whether the rankings induced by the empirical distances $\{\tau_i\}$ are correct with high probability. This was facilitated via a test which measures our "surprise" for measuring $\{\tau_i^\partial\}$ if the current estimate M is not correct with respect to Guarantee 1, which in turn used a test for how likely some candidate's $d(\mathbf{r}_i^*, \mathbf{r}_i^\partial)$ is greater than some threshold ε_i after taking n_i samples. We now provide a theorem that allows us to infer, given the samples taken for a given candidate, how to relate ε_i with the probability δ_i with which the candidate can fail to respect its deviation-bound ε_i. The bound seems to be known to the theoretical computer science community as a "folklore fact" [25]; we give a proof [51] for the sake of completeness. Our proof relies on repeated application of the method of bounded differences [52] in order to exploit some special structure in the ℓ_1 distance metric.

THEOREM 1. *Suppose we have taken* n_i *samples with replacement for some candidate* i*'s histogram, resulting in the empirical estimate* $\mathbf{r}_i$*. Then* $\mathbf{r}_i$ *has* ε_i*-deviation with probability greater than* $1 - \delta_i$ *for* $\varepsilon_i = \sqrt{\frac{2}{n_i}\left(|V_X| \log 2 + \log \frac{1}{\delta_i}\right)}$*. That is, with probability* $> 1 - \delta_i$*, we have:* $||\bar{\mathbf{r}}_i - \bar{\mathbf{r}}_i^*||_1 < \varepsilon_i$*.*

In fact, this theorem also holds if we sample without replacement; we return to this point in Section 4.

Optimality of the bound in Theorem 1. If we solve for n_i in Theorem 1, we see that we must have $n_i = \frac{|V_X| \log 4 + 2\log(1/\delta_i)}{\varepsilon_i^2}$. That is, $\Omega\left(\frac{|V_X|}{\varepsilon_i^2}\right)$ samples are necessary guarantee that the empirical discrete distribution $\bar{\mathbf{r}}_i$ is no further than ε_i from the true discrete distribution $\bar{\mathbf{r}}_i^*$, with high probability. This matches the information theoretical lower bound noted in prior work [12, 18, 24, 66].

3.4.4 Stage 2 Correctness

We now formally state the correctness of HistSim stage 2 [51].

LEMMA 5 (STAGE 2 CORRECTNESS). *After* HistSim *stage 2 completes, each candidate* $i \in M$*, satisfies* $\tau_i^* - \tau_j^* \le \varepsilon$ *for every* $j \in A \setminus M$ *with probability greater than* $1 - \frac{\delta}{3}$.

3.5 Stage 3 and Overall Proof of Correctness

Stage 3 of HistSim, discussed in our overall proof of correctness, consists of taking samples from each candidate in M to ensure they all have ε-deviation with high probability (using Theorem 1). This proof can be found in [51]; it proceeds in four steps:

- Step 1: HistSim stage 1 incorrectly prunes one or more candidates meeting the selectivity threshold σ with probability at most $\frac{\delta}{3}$ (Lemma 1).
- Step 2: The probability that stage 2 incorrectly (with respect to Guarantee 1) separates M and $A \setminus M$ is at most $\frac{\delta}{3}$.
- Step 3: The probability that the set of candidates M violates Guarantee 2 after stage 3 runs is at most $\frac{\delta}{3}$.
- Step 4: The union bound over any of these bad events occurring gives an overall error probability of at most δ.

THEOREM 2. *The* k *histograms returned by Algorithm 1 satisfy Guarantees 1 and 2 with probability greater than* $1 - \delta$.

Computational Complexity. Stage 1 of Algorithm 1 shares computation between candidates when computing P-values induced by the hypergeometric distribution, and thus makes at most $\max_{i\in V_Z} n_i$ calls to evaluate a hypergeometric pdf (we use Boost's implementation [1]); this can be done in $\mathcal{O}(\max_{i\in V_Z} n_i)$. To facilitate the sharing, stage 1 requires sorting the candidates in increasing order of n_i, which is $\mathcal{O}(|V_Z| \cdot \log |V_Z|)$. Next, each iteration of HistSim stage 2 requires computing distance estimates τ_i and τ_i^∂ for every $i \in A$, which runs in time $\mathcal{O}(|A| \cdot |V_X|)$. Each iteration of stage 2 further uses a sort of candidates in A by τ_i to determine M and s, which is $\mathcal{O}(|A| \cdot \log |A|)$. HistSim stage 2 almost always terminates within 4 or 5 iterations in practice. Overall, we observe that the computation required is inexpensive compared to the cost of I/O, even for data stored in-memory.

4. THE FASTMATCH SYSTEM

This section describes FastMatch, which implements the HistSim algorithm. We start by presenting the high-level components of FastMatch. We then describe the challenges we faced while implementing FastMatch and describe how the components interact to alleviate those challenges, while still satisfying Guarantees Guarantee 1 and Guarantee 2. While design choices presented in this section are heuristics with practicality in mind, the algorithm implemented is still theoretically rigorous, with results satisfying our probabilistic guarantees. In the following, each time we describe a heuristic, we will clearly point it out as such.

4.1 FastMatch Components

FastMatch has three key components: the I/O Manager, the Sampling Engine, and the Statistics engine. We describe each of them in turn; Figure 3 provides an architecture diagram—we will revisit the interactions within the diagram at the end of the section.

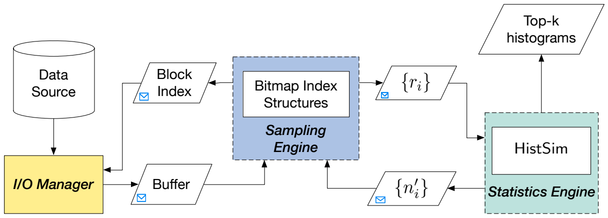

Figure 3: FastMatch system architecture

I/O Manager. In FastMatch, requests for I/O are serviced at the granularity of *blocks*. The I/O manager simply services requests for blocks in a synchronous fashion. Given the location of some block, it synchronously processes the block at that location.

Sampling Engine. The sampling engine is responsible for deciding which blocks to sample. It uses bitmap index structures (described below) in order to determine the types of samples located at a given block. Given the current state of the system, it prioritizes certain candidates over others for sampling.

Statistics Engine. The statistics engine implements most of the logic in the HistSim algorithm. The only substantial difference between the actual code and the pseudocode presented in Algorithm 1 is that the statistics engine does not actually perform any sampling, instead leaving this responsibility to the sampling engine. The reason for separating these components will be made clear later on.

Bitmap Index Structures. FastMatch runs on top of a bitmap-based sampling system used for sampling on-demand, as in prior work [8, 43, 42, 60]. These papers have demonstrated that bitmap indexes [17] are effective in supporting sampling for incremental or early termination of visualization generation. Within FastMatch, bitmap indexes help the sampling engine determine whether a given block contains samples for a given candidate. For each attribute A, and each attribute value A_v, we store a bitmap, where a '0' at position p indicates that the corresponding block at position p contains no tuples with attribute value A_v, and a '1' indicates that block p contains one or more tuples with attribute value A_v. Candidate visualizations are generated by attribute values, so these bitmaps allow the sampling engine to rapidly test whether a block contains tuples for a given candidate histogram. Bitmaps are amenable to significant compression [67, 68], and since we are further only requiring a single bit per block per attribute value, our storage requirements are orders-of-magnitude cheaper than past work that requires a bit per tuple [8, 42, 60].

4.2 Implementation Challenges

So far, we have designed HistSim without worrying about how sampling actually takes place, with an implicit assumption that there is no overhead to taking samples randomly across various candidates. While implementing HistSim within FastMatch, we faced several non-trivial challenges, outlined below:

Challenge 1: Random sampling at odds with performance characteristics of storage media. The cost to fetch data is locality-dependent when dealing with real storage devices. Even if the data is stored in-memory, tuples (i.e., samples) that are spatially closer to a given tuple may be cheaper to fetch, since they may already be present in CPU cache.

Challenge 2: Deciding how many samples to take between rounds of HistSim. The HistSim algorithm does not specify how many samples to taken in between rounds of stage 2; it is agnostic to this choice, with correctness unaffected. If the algorithm takes many samples, it may spend more time on I/O than is necessary to terminate with a guarantee. If the algorithm does not take enough samples, the statistical test on line 24 will probably not reject across many rounds, decaying δ^{upper} and making it progressively harder to get enough samples to meet stage 2's termination criterion.

Challenge 3: Non-uniform cost/benefit of different candidates. Tuples for some candidates can be over-represented in the data and therefore take less time to sample compared to underrepresented candidates. At the same time, the benefit of sampling tuples corresponding to different candidate histograms is non-uniform: for example, those histograms which are "far" from the target distribution are less useful (in terms of getting HistSim to terminate quickly) than those for which HistSim chooses small values for ε_i.

Challenge 4: Assessing benefit to candidates depends on data seen so far. The "best" choice of which tuples to sample for getting HistSim to terminate quickly can be most accurately estimated from *all* the data seen so far, including the most recent data. However, computing this estimate after processing every tuple (and thus constantly blocking I/O) is prohibitively expensive.
We now describe our approaches to tackling these three challenges.

Challenge 1: Randomness via Data Layout

To maximize performance benefits from locality, we randomly permute the tuples of our dataset as a preprocessing step, and to "sample" we may then simply perform a linear scan of the shuffled data starting from any point. This matches the assumptions of stage 1 of HistSim, which requires samples to be taken without replacement. Although the theory we developed in Section 3 for HistSim stage 2 was for sampling with-replacement, as noted in [32, 11], it still holds now that we are sampling without replacement, as concentration results developed for the with-replacement regime may be transferred automatically to the without-replacement regime. This approach of randomly permuting upfront is not new, and is adopted by other approximate query processing systems [69, 59, 71].

Challenge 2: Deciding Samples to Take Between Rounds

The HistSim algorithm leaves the number of samples to take during a given round of stage 2 lines 19 unspecified; its correctness is guaranteed regardless of how this choice is made. This choice offers a tradeoff: take too many samples, and the system will spend a lot of time unnecessarily on I/O; take too few, and the algorithm will never terminate, since the "difficulty" of the test increases with each round, as we set $\delta^{upper} \leftarrow \delta^{upper}/2$.

To combat this challenge, we employ a simple heuristic; the full description of which may be found in [51]. In brief, our sampling policy is informed by the statistical test on lines 20–23 — for each candidate i, we attempt to choose a number of samples to take n_i' that will cause this test to reject. We accomplish this by "inverting the bound" of Theorem 1. We emphasize that this dependency does not compromise the correctness of our results thanks to the union bound between rounds of stage 2 (see Theorem 2) and since each round's test uses fresh samples to compute the test statistics $\{\tau_i^{\partial}\}$.

Challenge 3: Block Choice Policies

During stage 1 of HistSim, we simply scan each block sequentially, as we are only trying to detect low-selectivity candidates. Deciding which blocks to read during stage 2 of HistSim is more difficult due to the non-uniform cost (i.e., time) and benefit of samples for each candidate histogram. Due to nonuniform cost, we cannot simply read in the blocks with the most beneficial candidates, and due to nonuniform benefit, we cannot simply read in the lowest cost blocks (e.g., those closest spatially to the current read position). Instead, we employ a simple policy which we found worked well in practice for getting HistSim to terminate quickly.

AnyActive **block selection policy.** Recall that the end of each iteration of stage 2 of HistSim estimates the number of samples $\{n_i'\}$

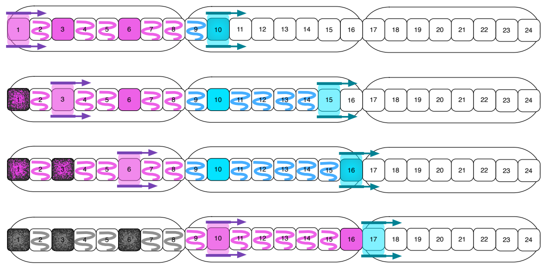

Figure 4: While the I/O manager processes magenta blocks, the sampling engine selects blue blocks ahead of time, using lookahead. Blocks with solid color = read, blocks with squiggles = skip.

necessary from each candidate so that the next iteration is more likely to terminate. Note that if each candidate satisfied $n_i = n'_i$ at the time HistSim performed the test for termination and *before* it computed the $\{n'_i\}$, then HistSim would be in a state where it can safely terminate. Those candidates for whom $n_i < n'_i$ we dub *active candidates*, and we employ a very simple block selection policy, dubbed the AnyActive block selection policy, which is to *only read blocks which contain at least one tuple corresponding to some active candidate*. The bitmap indexes employed by FastMatch allow it to rapidly test whether a block contains tuples for a given candidate visualization, and thus to rapidly apply the AnyActive block selection policy. Overall, our approach is as follows: we read blocks in sequence, and if blocks satisfy our AnyActive criterion, then we read all of the tuples in that block, else, we skip that block. We discuss how to make this approach performant below.

Challenge 4: Asynchronous Block Selection

From the previous discussion, the sampling engine employs an AnyActive block selection policy when deciding which blocks to process. Ideally, the $\{n_i\}$ and $\{n'_i\}$ (number of samples taken for candidate i and estimated number of samples needed for candidate i, respectively) used to assign active status to candidates should be computed from the freshest possible counts available to the sampling engine. That is, in an ideal setting, each candidate's active status would be updated immediately after each block is read, and the potentially new active status should be used for making decisions about immediately subsequent blocks. Unfortunately, this requirement is at odds with real system characteristics. Employing it exactly implies leaving the I/O manager idle while the sampling engine determines whether each block should be read or skipped. To prevent this issue, we relax the requirement that the sampling thread employ AnyActive with the freshest $\{n_i\}$ available to it. Instead, given the current $\{n_i\}$ and fresh set of $\{n'_i\}$, it precomputes the active status for each candidate and "looks ahead", marking an entire batch of blocks for either reading or skipping, and communicates this with the I/O manager. The batch size, or the lookahead amount, is a system parameter, and offers a trade-off between freshness of active states used for AnyActive and degree to which the I/O manager must idle while waiting for instructions on which block to read next. We evaluate the impact of this parameter in our experimental section. The lookahead process is depicted in Figure 4 for a value of lookahead $= 8$. While the I/O manager processes a previously marked batch of magenta-colored lookahead blocks, the sampling engine's lookahead thread marks the next batch in blue. It waits to mark the next batch until the I/O manager "catches up".

Employing lookahead allows us to prevent two bottlenecks. First, the sampling engine need not wait for each candidate's active status to update after a block is read before moving on to the next block, effectively decoupling it from the I/O manager. The second bottleneck prevented by lookahead is more subtle. A detailed description, with comparisons and pseudocode can be found in our technical report [51]. Here, we simply provide a high-level idea.The AnyActive block policy algorithm works by considering each candidate in turn, and querying a bitmap index for that candidate to determine whether the current block contains tuples corresponding to that candidate. Querying a bitmap actually brings in surrounding bits into the cache of the CPU performing the query, and evicts whatever was previously in the cache line. If blocks are processed individually, then only a single bit in the bitmap is used each time a portion is brought into cache. This is quite wasteful and turns out to hurt performance significantly as we will see in the experiments. Instead, applying AnyActive selection to lookahead-size chunks instead of individual blocks is a better approach. This approach has much better cache performance, since it allows an entire cache-line's worth of bits to be used. We verify the benefits of these optimizations in our experiments.

Table 2: Descriptions of Datasets

Dataset	Size	#Tuples	#Attributes	Replications
FLIGHTS	32 GiB	606 million	7	5×
TAXI	36 GiB	679 million	7	4×
POLICE	34 GiB	448 million	10	72×

4.3 System Architecture

FastMatch is implemented within a few thousand lines of C++. It uses pthreads [55] for its threading implementation. FastMatch uses a column-oriented storage engine, as is common for analytics tasks. We can now complete our description of Figure 3. When the I/O manager receives a request for a block at a particular block index from the sampling engine (via the "block index" message), it eventually returns a buffer containing the data at this block to the sampling engine (via the "buffer" message). Once the I/O phase of stage 1 or 2 of HistSim completes, the sampling engine sends the current per-group counts for each candidate, $\{\mathbf{r}_i\}$, to the statistics engine. After running a test for whether to move to stage 2 (performed in stage 1) or to terminate (performed in stage 2), the statistics engine either posts a message of updated n' (in stage 1) or $\{n'_i\}$ (stage 2) that the sampling engine uses to determine when to complete the I/O phase of each HistSim stage, as well as how to perform block selection during stage 2.

5. EXPERIMENTAL EVALUATION

The goal of our experimental evaluation is to test the accuracy and runtime of FastMatch against other approximate and exact approaches on a diverse set of real datasets and queries. Furthermore, we want to validate the design decisions that we made for FastMatch in Section 4 and evaluate their impact.

5.1 Datasets and Queries

We evaluate FastMatch on publicly available real-world datasets summarized in Table 2 — flight records [2], taxi trips [3], and police road stops [4]. The replication value indicates how many times each dataset was replicated to create a larger dataset. In preprocessing these datasets, we eliminated rows with "N/A" or erroneous values for any column appearing in one or more of our queries. Details on the datasets and attributes can be found in our technical report.

We evaluate several queries on each dataset, whose templates are summarized in Table 3. We had four queries on FLIGHTS, FLIGHTS-q1-q4, two on TAXI, TAXI-q1-q2, and three on POLICE, POLICE-q1-q3. For each query, the visual target was chosen to correspond with the closest distribution (under ℓ_1) to uniform, out of all histograms generated via the query's template, except for q1, q2, and q3 of FLIGHTS. Our queries spanned a number of interesting dimensions: *(i) frequently-appearing top-k candidates:*

Table 3: Summary of queries

Query	Z ($|V_Z|$)	X ($|V_X|$)	k	target
F-q_1	Origin (347)	DepartureHour (24)	10	Chicago ORD
F-q_2	Origin (347)	DepartureHour (24)	10	Appleton ATW
F-q_3	Origin (347)	DayOfWeek (7)	5	$1/[4, 8, 8, 8, 8, 8]$
F-q_4	Origin (347)	Dest (351)	10	closest $\bar{\mathbf{r}}_i$ to uniform
T-q_1	Location (7641)	HourOfDay (24)	10	closest $\bar{\mathbf{r}}_i$ to uniform
T-q_2	Location (7641)	MonthOfYear (12)	10	closest $\bar{\mathbf{r}}_i$ to uniform
P-q_1	RoadID (210)	ContrabandFound (2)	10	closest $\bar{\mathbf{r}}_i$ to uniform
P-q_2	RoadID (210)	OfficerRace (5)	10	closest $\bar{\mathbf{r}}_i$ to uniform
P-q_3	Violation (2110)	DriverGender (2)	5	closest $\bar{\mathbf{r}}_i$ to uniform

FLIGHTS-q1, POLICE-q1 and q2, *(ii) rarely-appearing top-k candidates:* FLIGHTS-q2 and q3, *(iii) high-cardinality candidate attribute Z:* TAXI-q1 and q2 ($|V_Z| = 7641$), POLICE-q3 ($|V_Z| = 2110$), and *(iv): high-cardinality grouping attribute X:* FLIGHTS-q4 ($|V_X| = 351$). The taxi queries in particular stressed our algorithm's ability to deal with low-selectivity candidates, since more than 3000 locations have fewer than 10 total datapoints.

5.2 Experimental Setup

Approaches. We compare FastMatch against a number of less sophisticated approaches that provide the same guarantee as FastMatch. All approaches are parametrized by a minimum selectivity threshold σ, and all approaches except Scan are additionally parametrized by ε and δ and satisfy Guarantees 1 and 2 with probability greater than $1 - \delta$.

- SyncMatch($\varepsilon, \delta, \sigma$). This approach uses FastMatch, but the AnyActive block selection policy is applied without lookahead, synchronously and for each individual block. *By comparing this method with* FastMatch*, we quantify how much benefit we may ascribe to the* lookahead *technique.*
- ScanMatch($\varepsilon, \delta, \sigma$). This approach uses FastMatch, but without the AnyActive block selection policy. Instead, no blocks are pruned: it scans through each block in a sequential fashion until the statistics engine reports that HistSim's termination criterion holds. *By comparing this with* SyncMatch*, we quantify how much benefit we may ascribe to* AnyActive *block selection.*
- Scan(σ). This approach is a simple heap scan over the entire dataset and always returns correct results, trivially satisfying Guarantees 1 and 2. It exactly prunes candidates with selectivity below σ. *By comparing* Scan *with our above approximate approaches, we quantify how much benefit we may ascribe to the use of approximation.*

Environment. Experiments were run on single Intel Xeon E5-2630 node with 125 GiB of RAM and with 8 physical cores (16 logical) each running at 2.40 GHz, although we use at most 2 logical cores to run FastMatch components. The Level 1, Level 2, and Level 3 CPU cache sizes are, respectively: 512 KiB, 2048 KiB, and 20480 KiB. We ran Linux with kernel version 2.6.32. We report results for data stored in-memory, since the cost of main memory has decreased to the point that most interactive workloads can be performed entirely in-core. Each run of FastMatch or any other approximate approach was started from a random position in the shuffled data. We report both wall clock times and accuracy as the average across 30 runs with identical parameters, with the exception of Scan, whose wall clock times we report as the average over 5 runs. Where applicable, we used default settings of $m = 5 \cdot 10^5$, $\delta = 0.01$, $\varepsilon = 0.04$, $\sigma = 0.0008$, and lookahead $= 1024$. We set the block size for each column to 600 bytes, which we found to perform well; our results are not too sensitive to this choice.

5.3 Metrics

We use several metrics to compare FastMatch against our baselines in order to test two hypotheses: one, that FastMatch does indeed provide accurate answers, and two, that the system architecture developed in Section 4 does indeed allow for earlier termination while satisfying the separation and reconstruction guarantees.

Table 4: Summary of average query speedups and latencies

Query		Avg Speedup over Scan (raw time in (s))		
	Scan(s)	ScanMatch	SyncMatch	FastMatch
F-q1	12.26	27.74× (0.44)	25.53× (0.48)	**37.52**× (0.33)
F-q2	12.29	3.17× (3.87)	2.73× (4.51)	**10.11**× (1.21)
F-q3	11.62	4.76× (2.44)	3.14× (3.70)	**8.72**× (1.33)
F-q4	13.97	5.93× (2.36)	5.76× (2.43)	**8.15**× (1.71)
T-q1	13.09	4.89× (2.68)	0.32× (40.95)	**15.93**× (0.82)
T-q2	13.09	6.48× (2.02)	0.37× (35.60)	**17.38**× (0.75)
P-q1	8.57	5.72× (1.50)	5.14× (1.67)	**13.34**× (0.64)
P-q2	8.49	14.31× (0.59)	15.48× (0.55)	**36.11**× (0.24)
P-q3	8.65	9.25× (0.93)	1.53× (5.66)	**33.26**× (0.26)

Wall-Clock Time. Our primary metric evaluates the end-to-end time of our approximate approaches that are variants of FastMatch, as well as a scan-based baseline.

Satisfaction of Guarantees Guarantee 1 and Guarantee 2. Our δ parameter ($\delta = 0.01$), serves as an upper bound on the probability that either of these guarantees are violated. If this bound were tight, we would expect to see about one run in every hundred fail to satisfy our guarantees. We therefore count the number of times our guarantees are violated relative to the number of queries performed.

Total Relative Error in Visual Distance. In some situations, there may be several candidate histograms that are quite close to the analyst-supplied target, and choosing any one of them to be among the k returned to the analyst would be a good choice. We define the *total relative error in visual distance* (denoted by Δ_d) between the k candidates returned by FastMatch and the true k closest visualizations as: $\Delta_d(M, M^*, \mathbf{q}) = \frac{\sum_{i \in M} d(\mathbf{r}_i, \mathbf{q}) - \sum_{j \in M^*} d(\mathbf{r}^*_j, \mathbf{q})}{\sum_{j \in M^*} d(\mathbf{r}^*_j, \mathbf{q})}$ Note that here, M^* is computed by Scan and only considers candidates meeting the selectivity threshold. Since FastMatch and our other approximate variants have no recall requirements with respect to identifying low-selectivity candidates (they only have precision requirements), it is possible for $\Delta_d < 0$.

5.4 Empirical Results

Speedups and Error of FastMatch versus others.

Summary. All FastMatch variants we tested show significant speedups over Scan for at least one query, but only FastMatch shows consistently excellent performance, typically beating other approaches and bringing latencies for all queries near interactive levels; with an overall speedup ranging between **8× and 35×** over Scan. Further, the output of FastMatch **and all approximate variants satisfied Guarantees 1 and 2 across all runs for all queries.**

Average run times of FastMatch and other approaches, for all queries as well as speedups over Scan, are summarized in Table 4. We used default settings for all runs. The reported speedups are the ratio of the average wall time of Scan with the average wall time of each approach considered. Scan was generally slower than approximate approaches because it had to examine all the data. Then, we typically observed that ScanMatch and SyncMatch were pretty evenly matched, with ScanMatch usually performing slightly better, except in some pathological cases where it performed very poorly due to poor cache usage. FastMatch had better performance than either SyncMatch or ScanMatch, thanks to lookahead paired with AnyActive block selection. Overall, we observed that each of FastMatch's key innovations: the termination criterion, the block selection, and lookahead, all led to substantial performance improvements, with an overall speedup of up to **35**× over Scan.

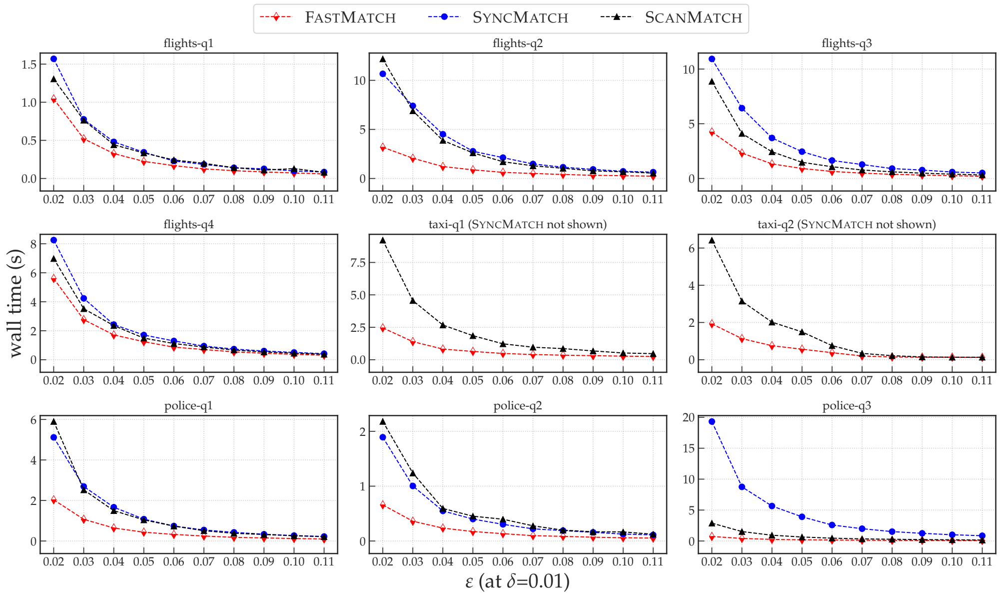

Figure 5: Effect of ε on query latency

Queries with high candidate cardinality (Taxi-q*, Police-q3), displayed particularly interesting performance differences. For these, FastMatch shows greatly improved performance over ScanMatch. It also scales much better to the large number of candidates than SyncMatch, which performs extremely poorly due to poor cache utilization and takes around $3\times$ longer than a simple non-approximate Scan. In this case, the `lookahead` technique of FastMatch is necessary to reap the benefits of AnyActive block selection.

Additionally, we found that the output of FastMatch *and all approximate variants satisfied Guarantees 1 and 2 across all runs for all queries.* This suggests that the parameter δ may be a loose upper bound for the actual failure probability of FastMatch.

Effect of varying ε.

Summary. In almost all cases, increasing the tolerance parameter ε leads to reduced runtime and accuracy, but **on average, Δ_d was never more than 5% larger than optimal for any query, even for the largest values of ε used.**

Figures 5 and 6 depict the effect of varying ε on the wall clock time and on Δ_d, respectively, using $\delta = 0.01$ and `lookahead` = 1024, averaged over 30 runs for each value of ε. Because of the extremely poor performance of SyncMatch on the Taxi queries, we omit it from both figures.

In general, as we increased ε, wall clock time decreased and Δ_d increased. In some cases, ScanMatch latencies matched that of Scan until we made ε large enough. This sometimes happened when it needed more refined estimates of the (relatively infrequent) top-k candidates, which it achieved by scanning most of the data, picking up lots of superfluous (in terms of achieving safe termination) tuples along the way.

Effect of varying `lookahead`. For most queries, we found that latency was relatively robust to changes in `lookahead`. Figure 7 depicts this effect. The queries with high candidate cardinalities (Taxi-q*, Police-q3) were the exceptions. For these queries, larger `lookahead` values led to increased utilization at all levels of CPU cache. Past a certain point, however, the performance gains were minor. Overall, we found the default value of 1024 to be acceptable in all circumstances.

Effect of varying δ. We refer readers to the technical report [51] for a full discussion (including experimental plots) on the effect of varying δ. In general, we found that increasing δ led to slight decreases in wall clock time, leaving accuracy (in terms of Δ_d) more or less constant. We believe this behavior is inherited from our bound in Theorem 1, which is not sensitive to changes in δ.

When approximation performs poorly. In order to achieve the competitive results presented in this section, the initial pruning of low-selectivity candidates during stage 1 of HistSim ended up being critical for good performance. With a selectivity threshold of $\sigma = 0$, stages 2 and 3 of HistSim are forced to consider many extremely rare candidates. For example, in the taxi queries, nearly half of candidates have fewer than 10 corresponding datapoints. In this case, ScanMatch performs the best (essentially performing a Scan with a slight amount of additional overhead), but it (necessarily) fails to take enough samples to establish Guarantees 1 and 2. SyncMatch and FastMatch likewise fail to establish guarantees, but additionally have the issue of being forced to consider many rare candidates while employing AnyActive block selection, which can slow town query processing by a factor of $100\times$ or more.

Comparing results for ℓ_1 and ℓ_2 metrics. So far, we have not validated our choice of distance metric (normalized ℓ_1); prior work has shown that normalized ℓ_2 is suitable for assessing the "visual" similarity of visualizations [65], so here, we compare our top-k with the top-k using the normalized ℓ_2 metric, for the Flights queries. In brief, we found that the relative difference in the total ℓ_1 distance of the top-k using the two metrics never exceeded 4% for any query, and that roughly 75% of the top-k candidates were common across the two metrics. Thus, ℓ_1 can serve as a suitable replacement for ℓ_2, while further benefiting from the advantages we described in Section 2. Please see [51] for the full discussion.

6. RELATED WORK

We now briefly survey work that is related to FastMatch.

Approximate Query Processing (AQP). Offline AQP involves computing a set of samples offline, and then using these samples when queries arrive e.g., [37, 19, 5, 9, 7], with systems like BlinkDB [7] and Aqua [6]. These techniques crucially rely on the availability of a workload. On the other hand, online approximate query processing, e.g., [31, 34, 48], performs sampling on-the-fly, typically using an index to facilitate the identification of appropriate samples. Our work falls into the latter category; however, none of the prior work has addressed a similar problem of identifying relevant visualizations given a query.

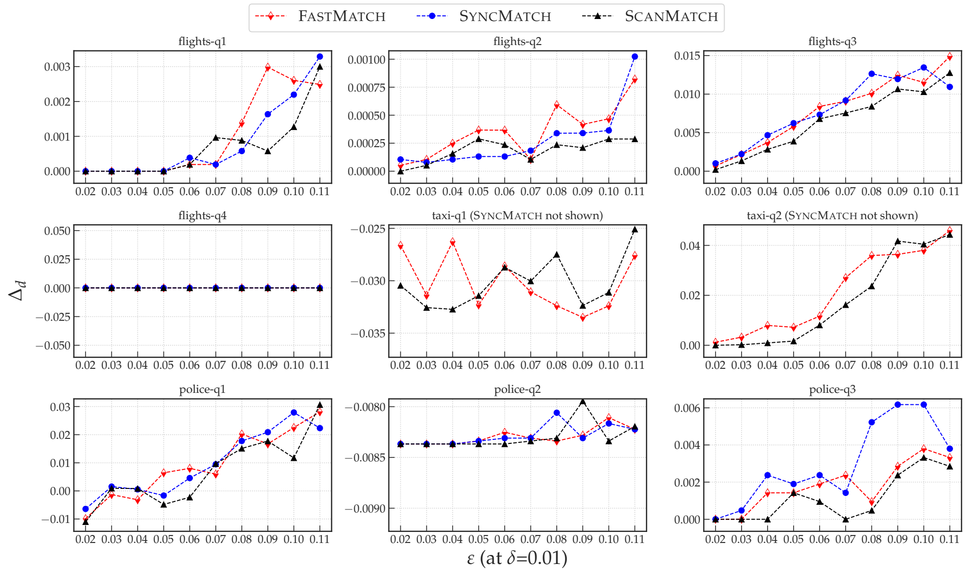

Figure 6: Effect of ε on Δ_d

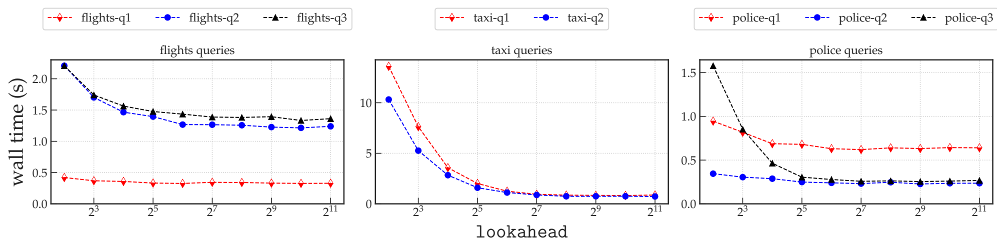

Figure 7: Effect of varying lookahead

Top-K or Nearest Neighbor Query Processing. There is a vast body of work on top-k query processing [35]. Most of this work relies on exact answers, as opposed to approximate answers, and has different objectives. Some work tries to bridge the gap between top-k query processing and uncertain query processing [64, 61, 63, 23, 57, 21, 44, 14], but does not need to deal with the concerns of where and when to sample to return answers quickly, but approximately. Some of this work [64, 61, 44, 14] develops efficient algorithms for top-k or nearest neighbors in a uncertain databases setting—here, the sampling is restricted to monte-carlo sampling, which is very different in behavior.

Scalable Visualizations. There has been some limited work on scalable approximate visualizations, targeting the generation of a single visualization, while preserving certain properties [42, 56, 60]. In our setting, the space of sampling is much larger—as a result the problem is more complex. Furthermore, the objectives are very different. Fisher et al. [27] explores the impact of approximate visualizations on users, adopting an online-aggregation-like [31] scheme. As such, these papers show that users are able to interpret and utilize approximate visualizations correctly. Some work uses pre-materialization for the purpose of displaying visualizations quickly [41, 46, 50]; however, these techniques rely on in-memory data cubes. We covered other work on scalable visualization via approximation [26, 53, 40, 56, 70, 65] in Section 1.

Histogram Estimation for Query Optimization. A number of related papers [20, 36, 38] are concerned with the problem of sampling for histogram estimation, usually for estimating attribute value selectivities [47] and query size estimation (see [22] for a recent example). While some of the theoretical tools used are similar, the problem is fundamentally different, in that the aforementioned line of work is concerned with estimating one histogram per table or view for query optimization purposes with low error, while we are concerned with comparing histograms to a specific target.

Sublinear Time Algorithms. HistSim is related to work on sublinear time algorithms—the most relevant ones [12, 18, 66] fall under the setting of distribution learning and analysis of *property testers* for whether distributions are close under ℓ_1 distance. Although Chan et al. [18] develop bounds for testing whether distributions are ε-close in the ℓ_1 metric, property testers can only say when two distributions p and q are equal or ε-far, and cannot handle $||p - q||_1 < \varepsilon$ for $p \neq q$, a necessary component of this work.

7. CONCLUSION

We developed sampling-based strategies for rapidly identifying the top-k histograms that are closest to a target. We designed a general algorithm, HistSim, that provides a principled framework to facilitate this search, with theoretical guarantees. We showed how the systems-level optimizations present in our FastMatch architecture are crucial for achieving near-interactive latencies consistently, leading to speedups ranging from $8\times$ to $35\times$ over baselines.

Acknowledgments. We thank the anonymous reviewers for their valuable feedback. We acknowledge support from grant IIS-1513407, IIS-1633755, IIS-1652750, and IIS-1733878 awarded by the National Science Foundation, and funds from Microsoft, Adobe, Toyota, Google, and the Siebel Energy Institute. Stephen Macke was sponsored by the National Science Foundation Graduate Research Fellowship grants NSF DGE-1144245 and NSF DGE-1746047. The content of this document is solely the responsibility of the authors and does not necessarily represent the official views of any funding agencies or other organizations.

8. REFERENCES

[1] Boost Statistical Distributions and Functions. https://www.boost.org/doc/libs/1_67_0/libs/math/doc/html/dist.html, 2006.

[2] Flight Records. http://stat-computing.org/dataexpo/2009/the-data.html, 2009.

[3] NYC Taxi Trip Records. https://github.com/toddwschneider/nyc-taxi-data/, 2015.

[4] WA Police Stop Records. https://stacks.stanford.edu/file/druid:py883nd2578/WA-clean.csv.gz, 2017.

[5] S. Acharya, P. B. Gibbons, and V. Poosala. Congressional samples for approximate answering of group-by queries. In *ACM SIGMOD Record*, volume 29, pages 487–498. ACM, 2000.

[6] S. Acharya, P. B. Gibbons, V. Poosala, and S. Ramaswamy. The aqua approximate query answering system. In *ACM Sigmod Record*, volume 28, pages 574–576. ACM, 1999.

[7] S. Agarwal, B. Mozafari, A. Panda, H. Milner, S. Madden, and I. Stoica. Blinkdb: Queries with bounded errors and bounded response times on very large data. In *EuroSys*, pages 29–42, New York, NY, USA, 2013. ACM.

[8] D. Alabi and E. Wu. Pfunk-h: approximate query processing using perceptual models. In *Proceedings of the 1st Workshop on Human-In-the-Loop Data Analytics*, page 10, 2016.

[9] N. Alon, Y. Matias, and M. Szegedy. The space complexity of approximating the frequency moments. In *STOC*, pages 20–29. ACM, 1996.

[10] B. Babcock, S. Chaudhuri, and G. Das. Dynamic sample selection for approximate query processing. In *SIGMOD*, New York, New York, USA, 2003.

[11] R. Bardenet, O.-A. Maillard, et al. Concentration inequalities for sampling without replacement. *Bernoulli*, 21(3):1361–1385, 2015.

[12] T. Batu, L. Fortnow, R. Rubinfeld, W. D. Smith, and P. White. Testing that distributions are close. In *FOCS*, 2000.

[13] J. T. Behrens. Principles and procedures of exploratory data analysis. *Psychological Methods*, 2(2):131, 1997.

[14] G. Beskales, M. A. Soliman, and I. F. Ilyas. Efficient search for the top-k probable nearest neighbors in uncertain databases. *PVLDB*, 1(1):326–339, 2008.

[15] G. Casella and R. L. Berger. *Statistical inference*, volume 2. Duxbury Pacific Grove, CA, 2002.

[16] K. Chakrabarti, M. Garofalakis, R. Rastogi, and K. Shim. Approximate query processing using wavelets. *PVLDB*, 10(2-3):199–223, 2001.

[17] C.-Y. Chan and Y. E. Ioannidis. Bitmap index design and evaluation. In *ACM SIGMOD Record*, volume 27, pages 355–366. ACM, 1998.

[18] S.-O. Chan, I. Diakonikolas, G. Valiant, and P. Valiant. Optimal algorithms for testing closeness of discrete distributions. In *SODA*, pages 1193–1203, 2014.

[19] S. Chaudhuri, G. Das, M. Datar, R. Motwani, and V. Narasayya. Overcoming limitations of sampling for aggregation queries. In *ICDE*, pages 534–542. IEEE, 2001.

[20] S. Chaudhuri, R. Motwani, and V. Narasayya. Random sampling for histogram construction: How much is enough? In *ACM SIGMOD Record*, volume 27, pages 436–447. ACM, 1998.

[21] C.-M. Chen and Y. Ling. A sampling-based estimator for top-k selection query. In *Data Engineering, 2002. Proceedings. 18th International Conference on*, pages 617–627. IEEE, 2002.

[22] Y. Chen and K. Yi. Two-level sampling for join size estimation. In *Proceedings of the 2017 ACM International Conference on Management of Data*, pages 759–774. ACM, 2017.

[23] E. Cohen, N. Grossaug, and H. Kaplan. Processing top-k queries from samples. *Computer Networks*, 52(14):2605–2622, 2008.

[24] C. Daskalakis, I. Diakonikolas, R. ODonnell, R. A. Servedio, and L.-Y. Tan. Learning sums of independent integer random variables. In *FOCS*, pages 217–226. IEEE, 2013.

[25] I. Diakonikolas. Personal communication, 2017.

[26] B. Ding, S. Huang, S. Chaudhuri, K. Chakrabarti, and C. Wang. Sample + seek: Approximating aggregates with distribution precision guarantee. In *SIGMOD*, 2016.

[27] D. Fisher, I. Popov, S. Drucker, and m.c. Schraefel. Trust me, i'm partially right. In *CHI*, page 1673, New York, New York, USA, may 2012. ACM Press.

[28] V. Ganti, M.-L. Lee, and R. Ramakrishnan. Icicles: Self-tuning samples for approximate query answering. *PVLDB*, pages 176–187, 2000.

[29] A. L. Gibbs and F. E. Su. On choosing and bounding probability metrics. *International statistical review*, 70(3):419–435, 2002.

[30] P. Hanrahan. Analytic database technologies for a new kind of user: The data enthusiast. In *SIGMOD*, pages 577–578, New York, NY, USA, 2012. ACM.

[31] J. M. Hellerstein, P. J. Haas, and H. J. Wang. Online aggregation. *ACM SIGMOD Record*, 26(2):171–182, jun 1997.

[32] W. Hoeffding. Probability inequalities for sums of bounded random variables. *Journal of the American statistical association*, 58(301):13–30, 1963.

[33] S. Holm. A simple sequentially rejective multiple test procedure. *Scandinavian journal of statistics*, pages 65–70, 1979.

[34] W.-C. Hou, G. Ozsoyoglu, and B. K. Taneja. Processing aggregate relational queries with hard time constraints. In *ACM SIGMOD Record*, volume 18, pages 68–77. ACM, 1989.

[35] I. F. Ilyas, G. Beskales, and M. A. Soliman. A survey of top-*k* query processing techniques in relational database systems. *ACM Comput. Surv.*, 40(4), 2008.

[36] Y. E. Ioannidis and V. Poosala. Balancing histogram optimality and practicality for query result size estimation. In *ACM SIGMOD Record*, volume 24, pages 233–244. ACM, 1995.

[37] Y. E. Ioannidis and V. Poosala. Histogram-based approximation of set-valued query-answers. *PVLDB*, pages 174–185, 1999.

[38] H. V. Jagadish, N. Koudas, S. Muthukrishnan, V. Poosala, K. C. Sevcik, and T. Suel. Optimal histograms with quality guarantees. pages 24–27, 1998.

[39] N. L. Johnson, A. W. Kemp, and S. Kotz. *Univariate discrete distributions*, volume 444. John Wiley & Sons, 2005.

[40] U. Jugel, Z. Jerzak, G. Hackenbroich, and V. Markl. M4: a visualization-oriented time series data aggregation. *PVLDB*, 7(10):797–808, 2014.

[41] S. Kandel, R. Parikh, A. Paepcke, J. M. Hellerstein, and J. Heer. Profiler: Integrated statistical analysis and visualization for data quality assessment. In *AVI*, pages 547–554. ACM, 2012.

[42] A. Kim, E. Blais, A. Parameswaran, P. Indyk, S. Madden, and R. Rubinfeld. Rapid sampling for visualizations with ordering guarantees. *PVLDB*, 8(5):521–532, 2015.

[43] A. Kim, L. Xu, T. Siddiqui, S. Huang, S. Madden, and A. Parameswaran. Optimally leveraging density and locality for exploratory browsing and sampling. In *Proceedings of the 3rd Workshop on Human-In-the-Loop Data Analytics*, pages 1–7, 2018.

[44] H.-P. Kriegel, P. Kunath, and M. Renz. Probabilistic nearest-neighbor query on uncertain objects. *Advances in databases: concepts, systems and applications*, pages 337–348, 2007.

[45] E. L. Lehmann and J. P. Romano. *Testing statistical hypotheses*. Springer Science & Business Media, 2006.

[46] L. D. Lins, J. T. Klosowski, and C. E. Scheidegger. Nanocubes for real-time exploration of spatiotemporal datasets. *IEEE TVCG*, 19(12):2456–2465, 2013.

[47] R. J. Lipton, J. F. Naughton, and D. A. Schneider. *Practical selectivity estimation through adaptive sampling*, volume 19. ACM, 1990.

[48] R. J. Lipton, J. F. Naughton, D. A. Schneider, and S. Seshadri. Efficient sampling strategies for relational database operations. *Theoretical Computer Science*, 116(1):195–226, 1993.

[49] Z. Liu and J. Heer. The effects of interactive latency on exploratory visual analysis. *IEEE TVCG*, 20(12):2122–2131, 2014.

[50] Z. Liu, B. Jiang, and J. Heer. immens: Real-time visual querying of big data. In *CGF*, volume 32, pages 421–430. Wiley Online Library, 2013.

[51] S. Macke, Y. Zhang, S. Huang, and A. Parameswaran. Fastmatch: Adaptive algorithms for rapid discovery of relevant histogram visualizations. Technical report, Available at: `http://data-people.cs.illinois.edu/papers/fastmatch.pdf`, 2017.

[52] C. McDiarmid. On the method of bounded differences. *Surveys in combinatorics*, 141(1):148–188, 1989.

[53] D. Moritz, D. Fisher, B. Ding, and C. Wang. Trust, but verify: Optimistic visualizations of approximate queries for exploring big data. In *CHI*, pages 2904–2915. ACM, 2017.

[54] B. Mozafari. Approximate query engines: Commercial challenges and research opportunities. In *SIGMOD*, pages 521–524. ACM, 2017.

[55] B. Nichols, D. Buttlar, and J. Farrell. *Pthreads programming: A POSIX standard for better multiprocessing*. " O'Reilly Media, Inc.", 1996.

[56] Y. Park, M. Cafarella, and B. Mozafari. Visualization-aware sampling for very large databases. In *ICDE*, pages 755–766. IEEE, 2016.

[57] A. Pietracaprina, M. Riondato, E. Upfal, and F. Vandin. Mining top-k frequent itemsets through progressive sampling. *Data Mining and Knowledge Discovery*, 21(2):310–326, 2010.

[58] P. Pirolli and S. Card. The sensemaking process and leverage points for analyst technology as identified through cognitive task analysis. In *Proceedings of international conference on intelligence analysis*, volume 5, pages 2–4, 2005.

[59] C. Qin and F. Rusu. Pf-ola: a high-performance framework for parallel online aggregation. *Distributed and Parallel Databases*, 32(3):337–375, 2014.

[60] S. Rahman, M. Aliakbarpour, H. K. Kong, E. Blais, K. Karahalios, A. Parameswaran, and R. Rubinfield. I've seen "enough": Incrementally improving visualizations to support rapid decision making. *PVLDB*, 10(11):1262–1273, 2017.

[61] C. Ré, N. N. Dalvi, and D. Suciu. Efficient top-k query evaluation on probabilistic data. In *ICDE*, pages 886–895, 2007.

[62] T. Siddiqui, A. Kim, J. Lee, K. Karahalios, and A. Parameswaran. Effortless data exploration with zenvisage: an expressive and interactive visual analytics system. *PVLDB*, 10(4):457–468, 2016.

[63] A. S. Silberstein, R. Braynard, C. Ellis, K. Munagala, and J. Yang. A sampling-based approach to optimizing top-k queries in sensor networks. In *Data Engineering, 2006. ICDE'06. Proceedings of the 22nd International Conference on*, pages 68–68. IEEE, 2006.

[64] M. A. Soliman, I. F. Ilyas, and K. C. Chang. Top-k query processing in uncertain databases. In *ICDE*, pages 896–905, 2007.

[65] M. Vartak, S. Rahman, S. Madden, A. Parameswaran, and N. Polyzotis. Seedb: efficient data-driven visualization recommendations to support visual analytics. *PVLDB*, 8(13):2182–2193, 2015.

[66] B. Waggoner. L p testing and learning of discrete distributions. In *ITCS*, pages 347–356. ACM, 2015.

[67] K. Wu, E. Otoo, and A. Shoshani. Compressed bitmap indices for efficient query processing. *Lawrence Berkeley National Laboratory*, 2001.

[68] K. Wu, K. Stockinger, and A. Shoshani. Breaking the curse of cardinality on bitmap indexes. In *Scientific and Statistical Database Management*, pages 348–365. Springer, 2008.

[69] S. Wu, B. C. Ooi, and K.-L. Tan. Continuous sampling for online aggregation over multiple queries. In *SIGMOD*, pages 651–662. ACM, 2010.

[70] Y. Wu, B. Harb, J. Yang, and C. Yu. Efficient evaluation of object-centric exploration queries for visualization. *PVLDB*, 8(12):1752–1763, 2015.

[71] K. Zeng, S. Agarwal, A. Dave, M. Armbrust, and I. Stoica. G-ola: Generalized on-line aggregation for interactive analysis on big data. In *SIGMOD*, pages 913–918. ACM, 2015.